Supporting information

In-Situ Derived $Ni_xFe_{1-x}OOH$/NiFe/$Ni_xFe_{1-x}OOH$ Nanotube Arrays from NiFe Alloys as Efficient Electrocatalysts for Oxygen Evolution

An-Liang Wang,[†§] Yu-Tao Dong,[†§] Mei Li,[‡] Chaolun Liang,[‡] and Gao-Ren Li[†]*

[†]*MOE Laboratory of Bioinorganic and Synthetic Chemistry, The Key Lab of Low-carbon Chemistry & Energy Conservation of Guangdong Province, School of Chemistry, Sun Yat-sen University, Guangzhou 510275, China*

[‡]*Instrumental Analysis and Research Centre, Sun Yat-sen University, Guangzhou 510275, China*

[§]These authors contributed equally to this work

E-mail: ligaoren@mail.sysu.edu.cn

EXPERIMENTAL SECTION

Fabrication of $Ni_xFe_{1-x}OOH$ /NiFe/$Ni_xFe_{1-x}OOH$ Nanotube Arrays

In this study, all the reagents were used without additional purification. Carbon fiber cloth (CFC) (2 cm× 0.5 cm) was firstly washed by ethanol and distilled water, respectively. The electrodeposition was carried out in a standard three-electrode cell. CFC, saturated calomel electrode (SCE) and graphite rod were used as working electrode, reference electrode and counter electrode, respectively. ZnO nanorod arrays (NRAs) were electrodeposited on the surface of CFC at the current density of 0.4 mA cm^{-2} at 70 ℃ for 1.5 h in the solution of 0.01 M NH_4NO_3+0.05 M $Zn(NO_3)_2$. After that, NiFe alloys was deposited on the surfaces of ZnO NRAs to achieve NiFe@ZnO NRAs in solution of 0.05 M Ni_2SO_4+0.05 M $FeSO_4$+0.2 M H_3BO_3 +0.05M sodium citrate at 25 ^{0}C. To optimize the composition of NiFe deposits, the total concentration of Ni^{2+} and Fe^{2+} in the electrolyte were maintained at 0.1 M, while the concentration ratio of Ni^{2+} and Fe^{2+} was systematically changed. Then NiFe@ZnO NRAs/CFC was immersed into the solution of 0.5 M KOH to etch ZnO for 5 h for the fabrication of NiFe alloy nanotube arrays (NTAs)/CFC (NiFe NTAs/CFC). Finally, NiFe-$Ni_xFe_{1-x}OOH$ NTAs supported on CFC (NiFe-$Ni_xFe_{1-x}OOH$ NTAs/CFC) were fabricated by a facile in-situ electrochemical oxidation of NiFe alloy NTAs during oxygen evolution. For comparative studies, Ni-NiOOH NTAs/CFC and Fe-FeOOH NTAs/CFC were also fabricated from Ni NTAs/CFC and Fe-OOH NTAs/CFC, respectively, via the similar methods. $NiFeO_x$ NTAs/CFC was obtained via the heat treatment of NiFe ANTAs/CFC at 500 ℃ for 4 h.

Structural characterizations

The surface morphologies were studied by field emission scanning electron microscope (SEM, FEI, Quanta 400, The accelerating voltages and working distances are 20 kV and 10 mm, respectively. The detector is backscattered electron detector) and transmission electron microscope (TEM, FEI Tecnai G2 F30, Cu grid is used as substrate). The high angle annular dark-field scanning transmission electron microscopy (HAADF-STEM) images and elemental mapping images of samples were also measured for samples. X-ray powder diffraction (XRD Bruker D8 Advance, Cu Kα radiation, scan rate is 5 ° min^{-1}) and selected

area electron diffraction (SAED) were used to study the phases and structures of materials. The chemical-state analysis of materials was analyzed by X-ray photoelectron spectroscopy (XPS, ESCALAB). For full spectrum, the passing energy is 100 eV and for high resolution curves, the passing energy is 20 eV, XPS spectra were corrected using C 1s line at 284.6 eV, and curve fitting and background subtraction were accomplished by Avantage software. The compositions of materials were determined using Inductively Coupled Plasma (ICP-AES).

Electrochemical Measurements

Electrochemical measurements were performed in 1.0 M KOH solution (purged with O_2 for 30 min) in a three-electrode system on CHI 760D electrochemical station. The NiFe-$Ni_xFe_{1-x}OOH$ NTAs/CFC, SCE and graphite rod were used as working electrode, reference electrode and counter electrode, respectively. All the potentials in this paper were referenced to a reversible hydrogen electrode (RHE) by following equation:

E(RHE)=E(SCE)+0.241+0.059 pH

The overpotential is calculated as follows:

$\eta = E$ (vs. RHE)-1.23

Considering O_2/H_2O equilibrium at 1.23 V vs. RHE

Electrochemical measurements of catalysts were measured in 1 M KOH solution (pH = 14) after purging the electrolyte with N_2 gas for 30 min at 25 °C. The electrocatalytic activity of NiFe-$Ni_xFe_{1-x}OOH$ NTAs/CFC (loading is 1.0 mg cm^{-2}) was measured by linear sweep voltammetry (LSV) at the scan rate of 2.0 mV cm^{-2}, and all polarization curves were IR-corrected. The chronopotentiometry is used to test the stability of NiFe ANTAs. EIS measurements were conducted at overpotential of 0.13 V in a frequency range from 100 kHz to 0.1 Hz to obtain the solution resistance (R_s), and all data were corrected with R_s. The TOF value was calculated by assuming that every metal atom in NiFe-$Ni_xFe_{1-x}OOH$ is involved in oxygen evolution reaction:

$$TOF = j \times A / 4F \times n \quad (1)$$

Where j is the measured geometric current density at overpotential of 350 mV, A is the surface area of electrode, the number 4 represents four electrons per mole of O_2, F is Faraday constant and n is the moles of metal atoms in NiFe-$Ni_xFe_{1-x}OOH$ ANTAs. For comparative studies, the same measurements of Ni-NiOOH NTAs and Fe-FeOOH NTAs, and $NiFeO_x$ NTAs were also conducted.

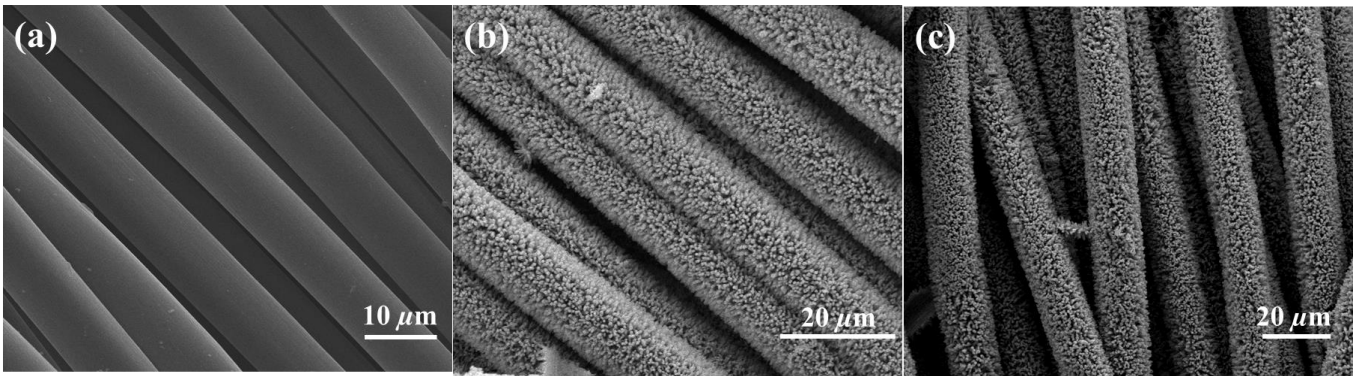

Figure S1. SEM images of (a) CFC, (b) ZnO NRAs/CFC and (c) NiFe@ZnO NRAs/CFC.

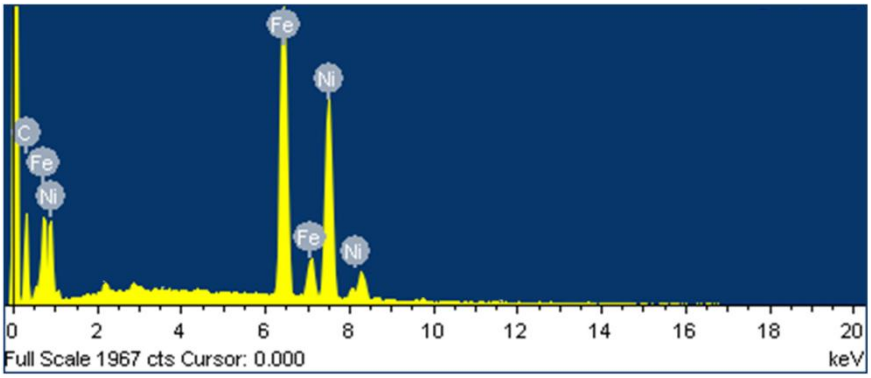

Figure S2. EDS spectrum of NiFe ANTAs/CFC.

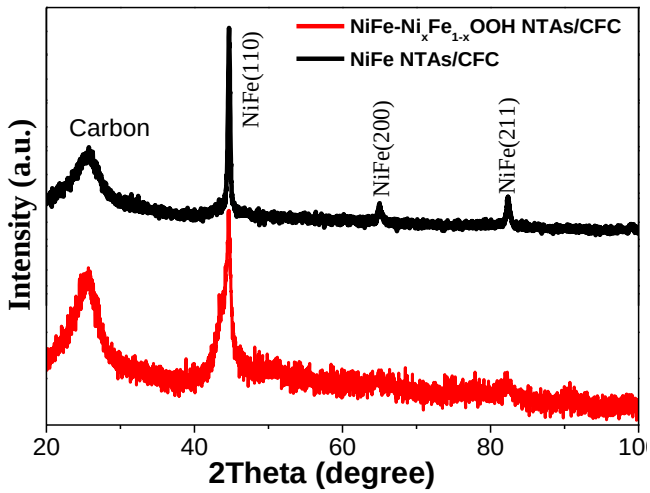

Figure S3. XRD patterns of NiFe ANTAs/CFC and NiFe-$Ni_xFe_{1-x}OOH$ NTAs/CFC.

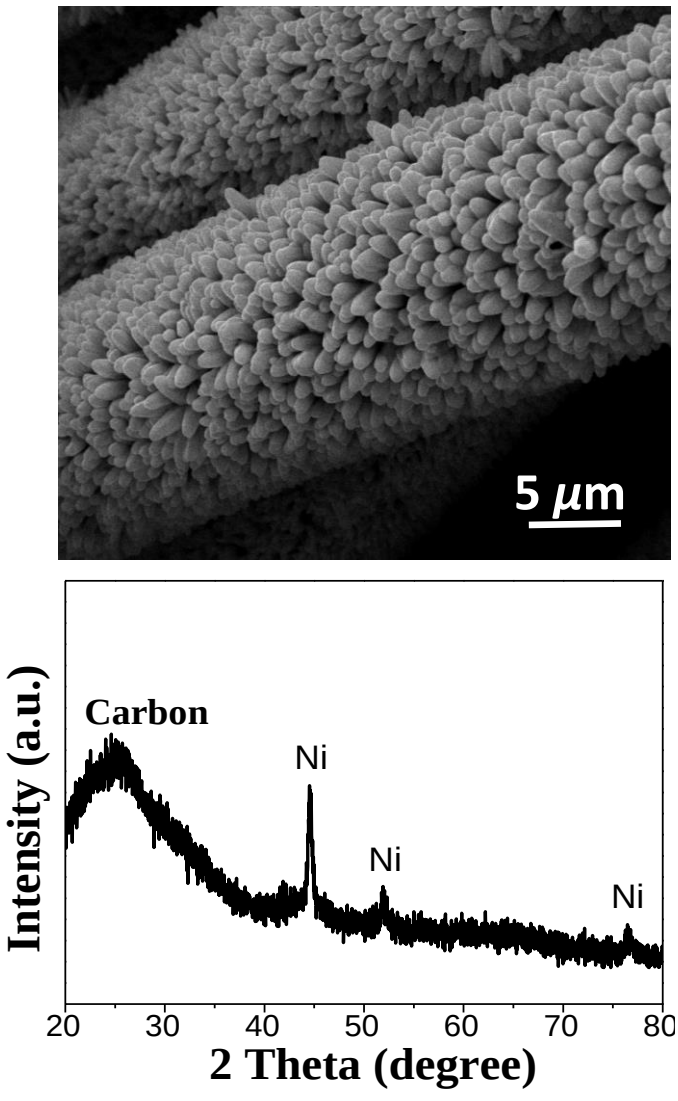

Figure S4. SEM image and XRD pattern of Ni-NiOOH NTAs/CFC.

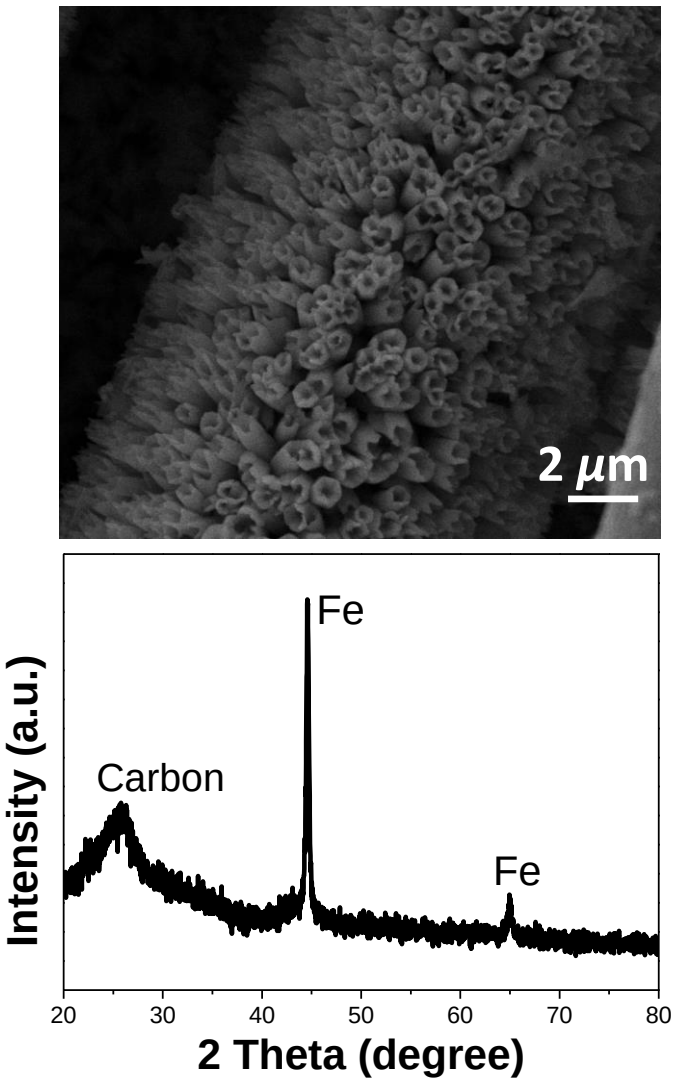

Figure S5. SEM image and XRD pattern of Fe-FeOOH NTAs/CFC.

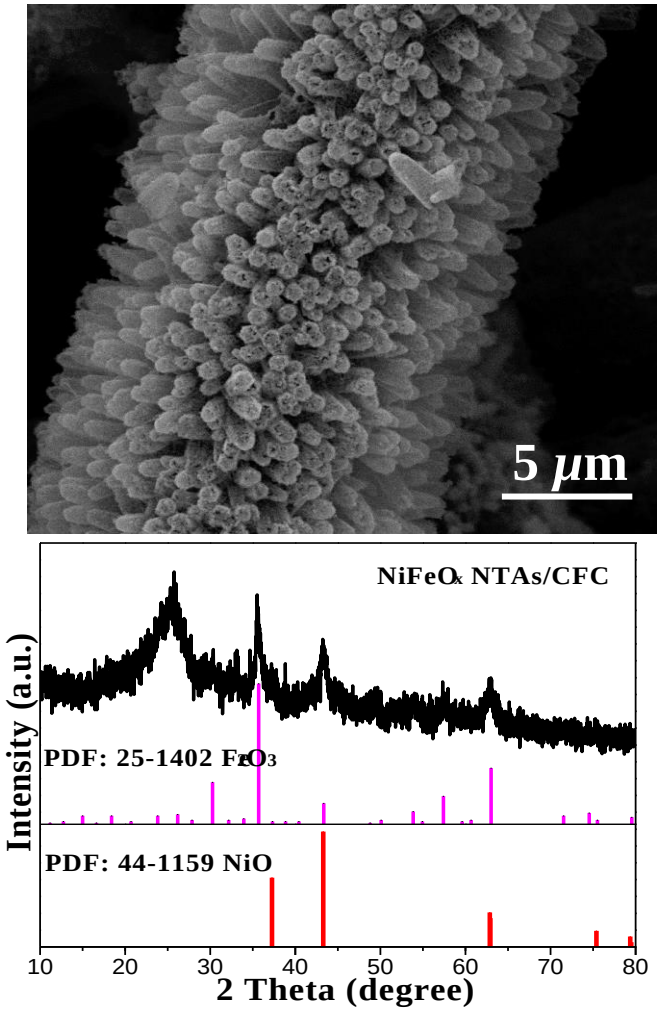

Figure S6. SEM image and XRD pattern of $NiFeO_x$ NTAs/CFC.

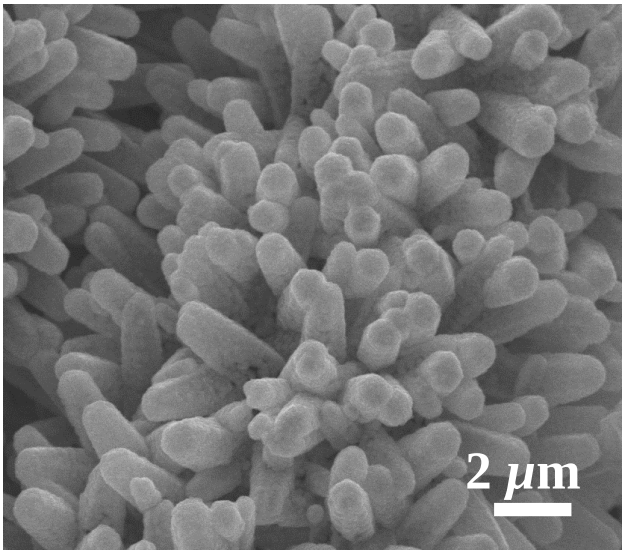

Figure S7. SEM image of NiFe-$Ni_xFe_{1-x}OOH$ NTAs/CFC after 30 h stability test.

Table S1. Surface concentrations for NiFe ANTAs-CFC before and after activation tests calculated from high resolution XPS.

Materials	Ni(%)	NiO(%)	NiOOH(%)	Fe(%)	Fe_2O_3(%)	FeOOH(%)
Before activation (Ni)	69	31	-	-	-	-
Before activation (Fe)	-	-	-	59	41	-
After activation (Ni)	-	-	100	-	-	-
After activation (Fe)	-	-	-	-	-	100

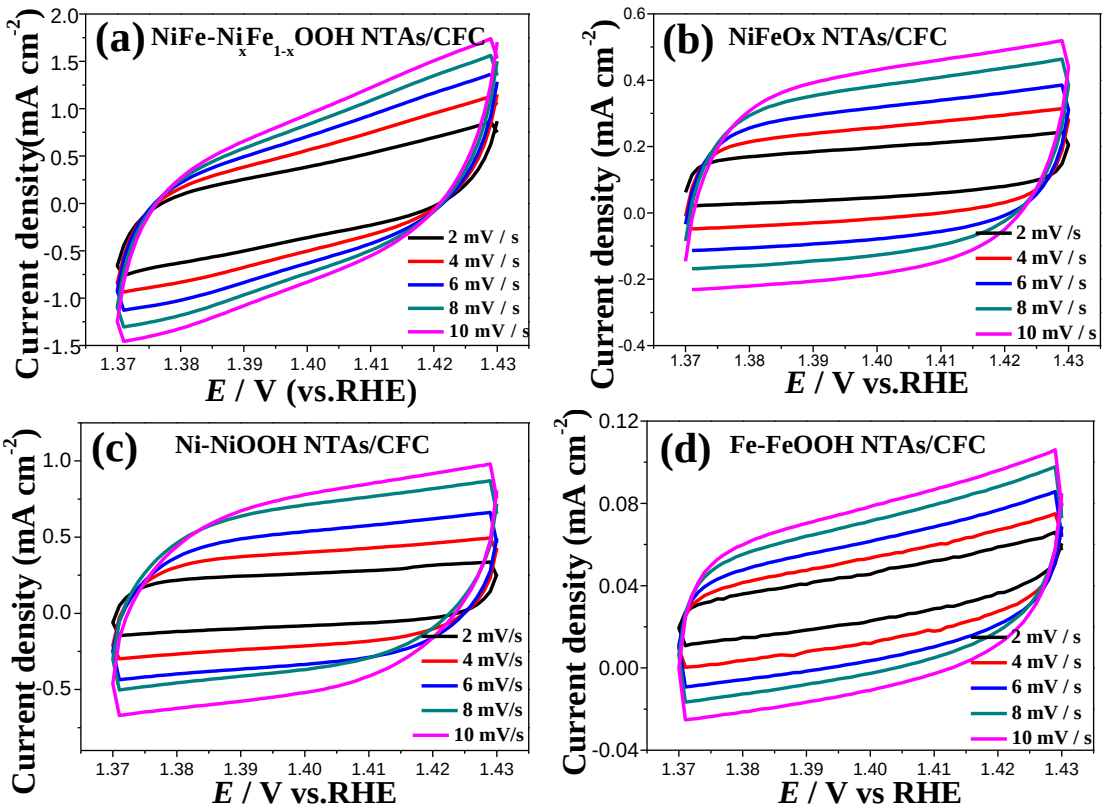

Figure S8. CV curves of (a) NiFe-Ni_xFe_{1-x}OOH NTAs/CFC, (b) $NiFeO_x$ NTAs/CFC, (c) Ni-NiOOH NTAs/CFC, and (d) Fe-OOH NTAs/CFC measured in 1.0 M KOH solution at scan rates of 2 to 10 mV s^{-1}.

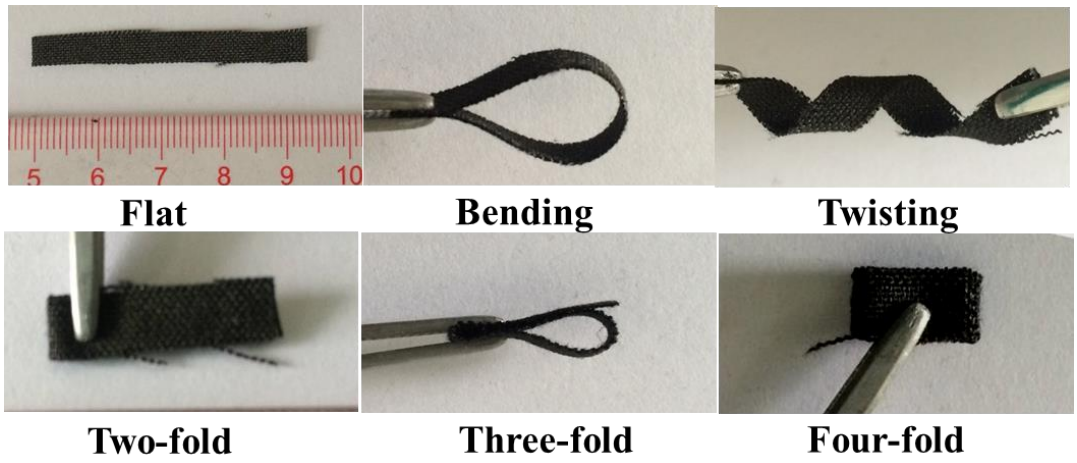

Figure S9. Optical images of NiFe-$Ni_xFe_{1-x}OOH$ ANTAs/CFC under different distorted states.

Table S2. Comparisons of OER electrocatalytic activity of NiFe ANTAs/CFC under alkaline conditions vis-à-vis other reported NiFe-based OER electrocatalysts.

Electrocatalysts	The overpotential at 10 mA cm^{-2} (V vs RHE)	Tafel slope (mV dec^{-1})	Loadings (mg cm^{-2})	Electrolyte	References
NiFe ANTAs/CFC	**220**	**57**	**1.0**	**1.0 M KOH**	**This work**
NiFe LDH/RGO	245	N.A.	1.0	1.0 M KOH	1
NiFe LDH/CNT	247	35	0.2	0.1 M KOH	2
NiFe LDH (exfoliated)	300	40	0.07	0.1 M KOH	3
NiFe LDH/RGO	206	39	0.25	1.0 M KOH	4
NiFe-LDH NP film	240	50	1.0	1.0 M KOH	5
CQD/NiFeLDH	235	30	0.2	1.0 M KOH	6
NiFe/C	250	30	0.36	1.0 M KOH	7
NiFeMo nanosheet	280	40	0.28	1.0 M KOH	8
NiFe LDH/oGSH	350	54	0.25	0.1 M KOH	9
NiFe MMO/CNT	230	45	0.28	1.0 M KOH	10
nNiFe LDH/NGF	337	45	0.25	0.1M KOH	11
NiFe/NF	240	33	0.032	0.1M KOH	12

N.A. refers to the unknown data.

References

1. Youn, D. H.; Park, Y. B.; Kim, J. Y.; Magesh, G.; Jang, Y. J.; Lee, J. S., One-Pot Synthesis of NiFe Layered Double Hydroxide/Reduced Graphene Oxide Composite as an Efficient Electrocatalyst for Electrochemical and Photoelectrochemical Water Oxidation. *J. Power Sources* **2015,** *294*, 437-443.
2. Gong, M.; Li, Y.; Wang, H.; Liang, Y.; Wu, J. Z.; Zhou, J.; Wang, J.; Regier, T.; Wei, F.; Dai, H., An Advanced Ni–Fe Layered Double Hydroxide Electrocatalyst for Water Oxidation. *J. Am. Chem. Soc* **2013,** *135* (23), 8452-8455.
3. Song, F.; Hu, X., Exfoliation of Layered Double Hydroxides for Enhanced Oxygen Evolution Catalysis. *Nat. Commun.* **2014,** *5*, 4477.
4. Long, X.; Li, J.; Xiao, S.; Yan, K.; Wang, Z.; Chen, H.; Yang, S., A Strongly Coupled Graphene and FeNi Double Hydroxide Hybrid as an Excellent Electrocatalyst for the Oxygen Evolution Reaction. *Angew. Chem.* **2014,** *126* (29), 7714-7718.
5. Lu, Z.; Xu, W.; Zhu, W.; Yang, Q.; Lei, X.; Liu, J.; Li, Y.; Sun, X.; Duan, X., Three-dimensional NiFe Layered Double Hydroxide Film for High-Efficiency Oxygen Evolution Reaction. *Chem. Commun.* **2014,** *50* (49), 6479-6482.
6. Tang, D.; Liu, J.; Wu, X.; Liu, R.; Han, X.; Han, Y.; Huang, H.; Liu, Y.; Kang, Z., Carbon Quantum Dot/NiFe Layered Double-hydroxide Composite as a Highly Efficient Electrocatalyst for Water Oxidation. *ACS Appl. Mater. Interfaces* **2014,** *6* (10), 7918-7925.
7. Feng, Y.; Zhang, H.; Zhang, Y.; Li, X.; Wang, Y., Ultrathin Two-Dimensional Free-Standing Sandwiched NiFe/C for High-Efficiency Oxygen Evolution Reaction. *ACS Appl. Mater. Interfaces* **2015,** *7* (17), 9203-9210.
8. Han, N.; Zhao, F.; Li, Y., Ultrathin Nickel–iron Layered Double Hydroxide Nanosheets Intercalated with Molybdate Anions for Electrocatalytic Water Oxidation. *J. Mater. Chem. A* **2015,** *3* (31), 16348-16353.
9. Zhu, X.; Tang, C.; Wang, H.-F.; Zhang, Q.; Yang, C.; Wei, F., Dual-Sized NiFe Layered Double Hydroxides in Situ Grown on Oxygen-Decorated Self-Dispersal Nanocarbon as Enhanced Water Oxidation Catalysts. *J. Mater. Chem. A* **2015,** *3* (48), 24540-24546.
10. Li, Y.; He, H.; Fu, W.; Mu, C.; Tang, X.-Z.; Liu, Z.; Chi, D.; Hu, X., In-grown Structure of NiFe Mixed Metal Oxides and CNT Hybrid Catalysts for Oxygen Evolution Reaction. *Chem. Commun.* **2016,** *52* (7), 1439-1442.
11. Tang, C.; Wang, H. S.; Wang, H. F.; Zhang, Q.; Tian, G. L.; Nie, J. Q.; Wei, F., Spatially Confined Hybridization of Nanometer-Sized NiFe Hydroxides into Nitrogen‐Doped Graphene Frameworks Leading to Superior Oxygen Evolution Reactivity. *Adv. Mater.* **2015,** *27* (30), 4516-4522.
12. Lu, X.; Zhao, C., Electrodeposition of Hierarchically Structured Three-dimensional Nickel–Iron Electrodes for Efficient Oxygen Evolution at High Current Densities. *Nat. Commun.* **2015,** *6*, 6616.